Atmospheric Trends and Radiative Forcings of CF 4 and C 2 F 6 Inferred from Firn Air

ARTICLE *in* ENVIRONMENTAL SCIENCE AND TECHNOLOGY · APRIL 2007

Impact Factor: 5.33 · DOI: 10.1021/es061710t · Source: PubMed

12 AUTHORS, INCLUDING:

David Robert Worton
National Physical Laboratory
86 PUBLICATIONS **910** CITATIONS
SEE PROFILE

L. K. Gohar
Met Office
29 PUBLICATIONS **752** CITATIONS
SEE PROFILE

David E. Oram
University of East Anglia
144 PUBLICATIONS **1,814** CITATIONS
SEE PROFILE

Robert Mulvaney
British Antarctic Survey
165 PUBLICATIONS **6,214** CITATIONS
SEE PROFILE

Environ. Sci. Technol. **2007**, *41,* 2184−2189

Atmospheric Trends and Radiative Forcings of CF_4 and C_2F_6 Inferred from Firn Air

DAVID R. WORTON,*,†,‖ WILLIAM T. STURGES,† LAILA K. GOHAR,‡ KEITH P. SHINE,‡ PATRICIA MARTINERIE,§ DAVID E. ORAM,† STEPHEN P. HUMPHREY,† PAUL BEGLEY,† LARA GUNN,†,§ JEAN-MARC BARNOLA,§ JAKOB SCHWANDER,& AND ROBERT MULVANEY#

School of Environmental Sciences, University of East Anglia, Norwich NR4 7TJ, U.K., Department of Meteorology, University of Reading, Reading RG6 6BB, U.K., CNRS Laboratoire de Glaciologie et Geophysique de l'Environnement, 38402 Saint Martin d' Heres cedex, France, Physics Institute, University of Bern, 3012 Bern, Switzerland, and British Antarctic Survey, Natural Environment Research Council, Cambridge CB3 0ET, U.K.

The atmospheric histories of two potent greenhouse gases, tetrafluoromethane (CF_4) and hexafluoroethane (C_2F_6), have been reconstructed for the 20th century based on firn air measurements from both hemispheres. The reconstructed atmospheric trends show that the mixing ratios of both CF_4 and C_2F_6 have increased during the 20th century by factors of ∼2 and ∼10, respectively. Initially, the increasing mixing ratios coincided with the rise in primary aluminum production. However, a slower atmospheric growth rate for CF_4 appears to be evident during the 1990s, which supports recent aluminum industry reports of reduced CF_4 emissions. This work illustrates the changing relationship between CF_4 and C_2F_6 that is likely to be largely the result of both reduced emissions from the aluminum industry and faster growing emissions of C_2F_6 from the semiconductor industry. Measurements of C_2F_6 in the older firn air indicate a natural background mixing ratio of <0.3 parts per trillion (ppt), demonstrating that natural sources of this gas are negligible. However, CF_4 was deduced to have a preindustrial mixing ratio of 34 ± 1 ppt (∼50% of contemporary levels). This is in good agreement with the previous work of Harnisch et al. (*18*) and provides independent confirmation of their results. As a result of the large global warming potentials of CF_4 and C_2F_6, these results have important implications for radiative forcing calculations. The radiative forcings of CF_4 and C_2F_6 are shown to have increased over the past 50 years to values in 2001 of 4.1×10^{-3} Wm^{-2} and 7.5×10^{-4} Wm^{-2}, respectively, relative to preindustrial concentrations. These forcings are small compared to present day forcings due to the major greenhouse gases but, if the current trends continue, they will continue to increase since both gases have essentially infinite lifetimes. There is, therefore, a large incentive to reduce perfluorocarbon emissions such that, through the implementation of the Kyoto Protocol, the atmospheric growth rates may decline in the future.

* Corresponding author phone: +1 510 643 0353; fax: +1 510 643 5098; e-mail: dworton@nature.berkeley.edu.
† University of East Anglia.
‡ University of Reading.
§ Laboratoire de Glaciologie et Géophysique de l'Environnement.
& University of Bern.
# British Antarctic Survey.
‖ Now at Division of Ecosystem Sciences, University of California, Berkeley, CA 94720-3110.
§ Now at School of Earth and Environment, University of Leeds, Leeds LS2 9JT, U.K.

Introduction

Tetrafluoromethane (CF_4) and hexafluoroethane (C_2F_6) are the most abundant perfluorocarbons (PFCs) in the contemporary atmosphere with reported mixing ratios of ∼78 and ∼3 parts per trillion (ppt), respectively (*1*−*4*). Both species strongly absorb infrared radiation in the "atmospheric window" region (*5*−*7*) and have long atmospheric lifetimes (Table 1) (*8*, *9*). These long lifetimes arise from their high stability in the atmosphere, with the only significant loss processes being photolysis and/or ion reactions in the mesosphere (*10*) and destruction in the high-temperature combustion zones of power plants and automobiles (*9*, *11*). The estimated 100 year global warming potentials for CF_4 and C_2F_6 are several thousand times larger than that of carbon dioxide (Table 1) (*8*), making these two species among the most potent greenhouse gases emitted on a per molecule basis as a result of human activity.

Primary aluminum production is recognized to be the major anthropogenic source of CF_4 and C_2F_6 (*8*, *12*−*14*). CF_4 and C_2F_6 are not emitted during normal operating conditions and only occur during brief upset conditions known as "anode effects" (*14*−*16*), which occur when the aluminum oxide level within the electrolytic bath drops below a critical threshold necessary for electrolysis. CF_4 and C_2F_6 have also been used as dry etching and plasma cleaning agents in the semiconductor industry since the early 1970s (*17*). They are emitted into the atmosphere as the result of fugitive emissions unless abatement technologies are employed to scrub the waste streams (*13*).

Harnisch et al. (*18*) have shown evidence for a CF_4 preindustrial background of ∼50% of contemporary mixing ratios from the analysis of air trapped in glacial ice. The estimated natural CF_4 flux of <0.01 Gg yr^{-1} (*4*, *18*), necessary to maintain a background of 39 ± 6 ppt, is believed to be geochemical in origin as a result of CF_4 emissions being detected following the heating, crushing, and aqueous dissolution of certain rocks and minerals (*19*, *20*). C_2F_6 was not observed to be released from these rock samples (*19*, *20*) and has previously been hypothesized to be entirely anthropogenic in origin (*21*). Neither species was observed to be present in volcanic degassing (*22*). The estimated natural flux of CF_4 is insignificant relative to the estimated anthropogenic flux of >10 Gg yr^{-1}, reportedly emitted by the aluminum industry (*23*).

Khalil et al. (*3*) have also shown evidence for a CF_4 preindustrial background of ∼44 ppt, within the reported uncertainties of Harnisch et al. (*18*). Khalil's estimate was based on extrapolating the CF_4:C_2F_6 relationship to zero C_2F_6 concentrations from ambient air samples collected at Cape Meares, Oregon, Point Barrow, Alaska, and Palmer Station, Antarctica, between 1978 and 1990. This period was recognized to be when the major source of these two gases was from aluminum smelting and before there was a significant

10.1021/es061710t CCC: $37.00
Published on Web 02/22/2007

TABLE 1. Atmospheric Lifetimes (*8*), Relative Global Warming Potentials (GWP) Used in the IPCC (*8*) and in This Work (*7*, *37*), and the Estimated Diffusion Coefficients, as Determined from Le Bas Molecular Volumes (*34*), Used in the Firn Modeling for CF_4 and C_2F_6

	lifetime (years)	GWP relative to CO_2(100 year time horizon); IPCC	GWP relative to CO_2(100 year time horizon); this work	diffusion coefficient relative to CO_2
CF_4	50000	5820[a]	7200[b]	0.711
C_2F_6	10000	12010[a]	12100[c]	0.595

[a] Reference *8*. [b] Reference *7*. [c] Reference *37*.

contribution from the semiconductor industry. Interestingly, as our results will show, the CF_4 to C_2F_6 slope has changed since 1990 providing evidence of the increased contribution of C_2F_6 emissions from the semiconductor industry. Our firn air measurements provide older air, which enables improved constraints on the natural CF_4 background estimation based on only the early gradient of CF_4 versus C_2F_6.

Experimental Approach

Firn Air Measurements and Modeling. Firn air samples were collected at the North Greenland ice core project site (NGRIP), Greenland (75° N, 42° W; 2001), and Berkner Island, Antarctica (80° S, 46° W; 2003). Details of the NGRIP (*24*) and Berkner Island sites (*25*), sampling procedures (*26*, *27*), and analytical methodologies (*26*, *28*, *29*) have been given elsewhere. More details of the analytical method are given in the Supporting Information (SI). The associated experimental uncertainties, as illustrated by the error bars in subsequent figures, were determined as the total analytical precision through duplicate analyses of samples at each depth and the measurement precision of the working standard (ambient air filled in the Colorado Mountains in 1994 by the National Oceanic and Aeronautical Administration—Climate Monitoring and Diagnostics Laboratory); see the SI.

The calibration was performed (CF_4, this work; C_2F_6 (*30*)) using a static dilution of the pure gases (*29*). Following this calibration, values of 72 ± 10 ppt CF_4 and 2.2 ± 0.22 ppt C_2F_6 were assigned to the working standard. The uncertainties in the assigned numbers reflect the absolute errors of the calibration including all systematic and random errors. The response of the mass spectrometer was observed to exhibit linearity across all concentrations. More details of the calibration procedure are given in the SI.

The measured concentration depth profiles were interpolated into atmospheric trends using an iterative approach (*31*) in conjunction with a firn physical transport model (*32*) that accounts for gravitational fractionation and gaseous diffusion within the firn. More details of this iterative modeling methodology are given in the SI. The required tortuosity profile for the firn modeling was determined by inverse modeling of the CO_2 profile (*33*). Diffusion coefficients of CF_4 and C_2F_6 relative to CO_2 (Table 1) were estimated from Le Bas molecular volumes (*34*). Thermal fractionation effects were not included in the model and are not believed to be significant. The best fit firn model outputs, for each gas at each site, are shown in Figure 1. These equate to the best estimate time trends discussed thereafter.

Data from the two deepest samples (61 and 63 m) at Berkner Island have been excluded from this work due to contamination issues as indicated by anomalously high CFC-113 and HCFC-142b concentrations in these samples. The contamination was believed to be the result of a leak in the pumping system at the surface that developed during the collection of these samples.

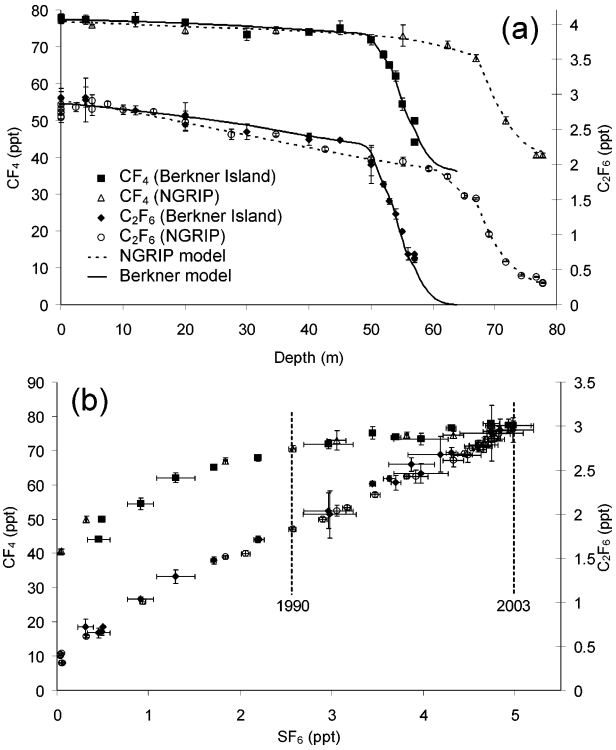

FIGURE 1. (a) Firn air concentration−depth profiles of CF_4 and C_2F_6 at NGRIP and Berkner Island. The solid and dashed lines are modeled best fits corresponding to the atmospheric scenarios shown in Figure 2. (b) CF_4 and C_2F_6 plotted against SF_6. The years 1990 and 2003, determined through iterative dating of SF_6 at NGRIP, are shown.

Radiative Forcing Calculations. The radiative forcing calculations were carried out using the Intergovernmental Panel on Climate Change (IPCC) formula (*35*). This involves multiplying the radiative efficiency (the radiative forcing per parts per billion per volume (Wm^{-2} $ppbv^{-1}$)) by the gas concentrations derived from the Laboratoire de Glaciologie et Géophysique de l'Environnement's 2D chemistry transport model (*36*). The radiative efficiencies used for CF_4 and C_2F_6 were 0.10 Wm^{-2} $ppbv^{-1}$ and 0.27 Wm^{-2} $ppbv^{-1}$, respectively. The efficiencies were calculated using spectral infrared absorption cross sections measured at the Ford Motor Company (Michigan) and radiative transfer codes (see ref *7* for CF_4 and ref *37*) for C_2F_6). This method can be used for long-lived gases such as CF_4 and C_2F_6, which have small variations in their vertical profiles. The difference in radiative forcing between assuming a constant vertical profile of concentration and a vertically varying profile was found to be $\leq$1% for CF_4 and C_2F_6. The CF_4 forcing has been shown to be sensitive to the amount of both CF_4 and other species that absorb in the same spectral region (*7*). We have used values appropriate to the present day atmosphere.

Results and Discussion

Figure 1 shows the CF_4 and C_2F_6 measurements at the NGRIP and Berkner Island sites versus depth (Figure 1a) and sulfur hexafluoride (SF_6) (Figure 1b). SF_6 was used to give an axis that is more linear with time and that allows comparisons between the two different sites. This is because SF_6 is very long-lived in the atmosphere, $\tau = 3200$ years (*8*), and has increased in both hemispheres at the same rate. By plotting CF_4 and C_2F_6 against SF_6 it is possible to more clearly illustrate the differing growth rates of CF_4 and C_2F_6 relative to SF_6, which increased exponentially in the atmosphere over the period 1970−1997 (*38*, *39*), as illustrated by the apparent leveling off of CF_4 at SF_6 concentrations >3 ppt (Figure 1b).

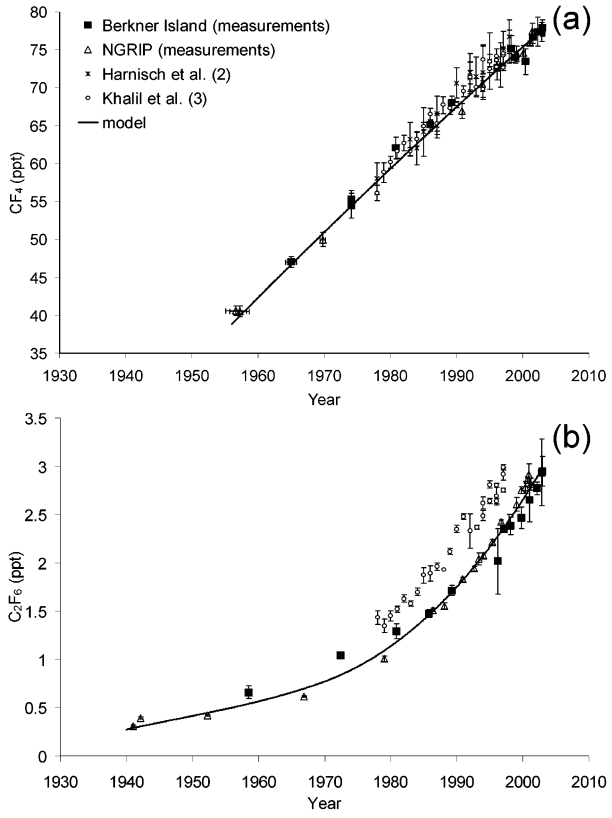

FIGURE 2. Atmospheric trends of (a) CF_4 and (b) C_2F_6 reconstructed from iterative modeling of the firn air profiles at NGRIP and Berkner Island. Solid lines are the average of the NGRIP and Berkner Island best fit trends for each gas. Data from Harnisch et al. (*2*) and Khalil et al. (*3*) are also shown.

There is excellent agreement for both CF_4 and C_2F_6 between both sites, as expected for very long-lived species that are well mixed throughout the atmosphere. Approximate dates at several depths in the profiles are also shown in Figure 1. These dates were determined through iterative modeling of the SF_6 data from NGRIP and are only approximate as a result of the differing diffusion rates for the different species through the firn, hence the requirement to use the firn modeling technique to determine time trends independently of SF_6 dating.

The reconstructed atmospheric trends of CF_4 and C_2F_6 (Figure 2) clearly show their increasing atmospheric burdens. The atmospheric abundance of CF_4 is observed to have increased by a factor of ~2 from 40 to 78 ppt between ~1955 and 2003 while C_2F_6 has increased by a factor of ~10 from 0.3 to 2.9 ppt between ~1940 and 2003. For CF_4, the uncertainties in the dating of the sampling depths, illustrated by *x*-axis error bars (Figure 2a), reflects the uncertainty in the estimation of the preindustrial CF_4 value (34 ± 1 ppt determined from Figure 3) used in the model runs.

Figure 2 also shows the measurements of Harnisch et al. (*2*) (CF_4) and Khalil et al. (*3*) (CF_4 and C_2F_6). There is excellent agreement of these two datasets with our firn air measurements for CF_4 (Figure 2a). Our C_2F_6 measurements are in reasonable agreement with those reported by Khalil et al. (*3*) (Figure 2b) although they are lower by ~20%. Harnisch et al. (*4*) showed C_2F_6 rising by a factor of ~2, from 1.5 to 2.6 ppt, between 1982 and 1995 broadly in agreement with our measurements. Khalil et al. (*3*) showed that there are significant calibration differences between the datasets of different groups. Therefore, we consider our results to be in approximate agreement with expectations and any observed differences in the absolute numbers between different datasets are likely to be the result of calibration uncertainties.

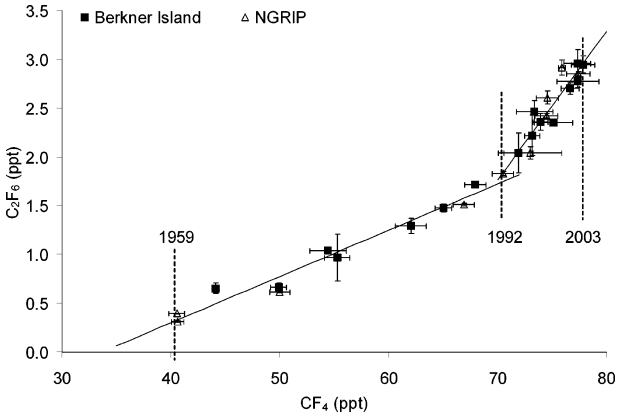

FIGURE 3. Changing relationship between CF_4 and C_2F_6 from NGRIP and Berkner Island firn air. The solid lines are best fit lines to the two obvious trends determined through a linear least-squares curve fitting routine.

The lowest mixing ratios of CF_4 and C_2F_6 observed from the firn measurements were 40 and 0.3 ppt, respectively (Figure 1). This strongly suggests that while CF_4 has a preindustrial background, natural emissions of C_2F_6 are negligible. The relationship between CF_4 and C_2F_6 was investigated by plotting them against each other (Figure 3). From this figure it is possible to estimate the natural background of CF_4 by extrapolating the early CF_4:C_2F_6 relationship (<1992) to zero C_2F_6 concentrations (Figure 3). Using a linear least-squares curve fitting routine a value of 34 ± 1 ppt was determined as the natural background of CF_4. This value is within the uncertainty range of 39 ± 6 ppt found by Harnisch et al. (*18*) but lower than the 44 ppt reported by Khalil et al. (*3*). The greater age range of the firn air measurements constrains this extrapolation leading to an improved value for the preindustrial CF_4 background relative to previous estimates.

It is clear from Figure 3 that the relationship between CF_4 and C_2F_6 has changed significantly during the last ~15 years, with the steeper gradient implying that the current atmospheric growth rate of C_2F_6 is greater than that of CF_4. Since the major atmospheric sources of these two PFC's are understood to be from aluminum smelting and semiconductor production, this result would suggest that the emissions of CF_4 and C_2F_6 from these two industries have recently changed.

Primary aluminum production has increased from a few thousand metric tonnes in 1900 to >23 million metric tonnes in 2003 (*23*, *40*) with the greatest increases occurring in the latter part of the century. As a result of both the environmental and economic benefits of reducing "anode effects", there has been an industry wide voluntary commitment to a variety of national level governmental PFC emission reduction programs. The International Aluminum Institute (IAI), which represents the majority of global aluminum producers (~80% in 2000), has undertaken a program called the "PFC emissions and anode effect survey" to evaluate the specific emissions from as many of the smelters that are in operation as possible, as described previously by Khalil et al. (*3*).

The PFC emissions reduction program (*15*) describes the newest technology, point feed prebake (PFPB), as being the smelter technology responsible for the majority of the current reported global aluminum production. The PFPB technology was not described or discussed in the previous Khalil et al. (*3*) publication. This technology incorporates multiple "point feeders" and other computerized controls for precise aluminum feeding, which minimizes the occurrence of "anode

effects" and reduces the production of CF_4 and C_2F_6. Another key feature of these production cells is their enclosed nature coupled with the presence of gas and particle scrubbers, which significantly reduce the fugitive emissions.

Since the early 1990s the quantity of aluminum being produced by smelters utilizing the PFPB technology has shown the largest growth in production output, increasing by a factor of 3 from ~5 million tonnes in 1990 to >15 million tonnes in 2003 (*40*). This increase is complemented by the decline in the emission factor (i.e., kg CF_4 emitted per tonne of aluminum produced) from PFPB smelters by a factor of >3 over the same time period. This means that, in 2003, while PFPB smelters accounted for over half of total global primary aluminum production they generate only around one-third of the PFC emissions (*40*).

CF_4 and C_2F_6 along with several other fluorinated species (e.g., C_3F_8, c-C_4F_8, SF_6, NF_3, and CHF_3) are critical to current semiconductor manufacturing methods because their unique characteristics when used in a plasma cannot be duplicated by alternatives. The industry's technical reliance on high global warming potential (GWP) gases increased significantly (~61%) from 1990−1997 (*13*). However, as a result of the initial implementation of PFC emission reduction methods such as process optimization and abatement technologies the emissions growth rate, for the United States at least, began to slow after 1997 and has reportedly declined during the period 1999−2004 by ~35% (*13*).

We hypothesize that the observed changing relationship between CF_4 and C_2F_6 (Figure 3) is the result of reduced emissions of CF_4 and C_2F_6 per tonne of aluminum produced and differing increases in the emissions of both species from the semiconductor industry. The Emissions Database for Global Atmospheric Research (EDGAR) has recently been updated (version 3.2) to incorporate emissions of the new "Kyoto" greenhouse gases (i.e., SF_6, PFCs, and the hydrofluorocarbons) for the period 1970−1998 (*41*). The estimated annual global emissions of CF_4 and C_2F_6 reported in EDGAR are shown in Figure 4 along with the global primary aluminum production (*23*). The estimated CF_4 emissions derived from the atmospheric trend in Figure 2 is shown as the solid line in Figure 4a. These emissions were determined by multiplying the annual concentration changes by the approximate conversion figure reported by Khalil et al. (*3*), i.e., 1 ppt yr^{-1} = 14.7 Gg yr^{-1} for CF_4. The reported conversion figure for C_2F_6, used in subsequent calculations, was 23 Gg yr^{-1} for 1 ppt yr^{-1} (*3*). In general, there is good agreement between our work and EDGAR for CF_4 (Figure 4a).

It is possible to make an estimation of the individual contribution of the aluminum and semiconductor industries to the total C_2F_6 emissions from the relationship observed in Figure 3. The early linear slope of CF_4 versus C_2F_6 can be assumed to be characteristic of the aluminum industry since there was no significant semiconductor production at this time and the natural emission rate is negligible. Therefore, the CF_4:C_2F_6 ratio can be calculated, assuming all CF_4 comes from aluminum smelting, for the years 1970−2001 from the early slope (Figure 3) giving a constant value of 13 ± 0.8 from our work, which is in reasonable agreement with the values of 10 from EDGAR and 10−12 used by Khalil et al. (*3*).

However, it is important to note that the different smelter designs have been observed to exhibit different CF_4:C_2F_6 emission ratios (*15*) and that the CF_4:C_2F_6 mass emission ratio has been estimated to have declined between 1970−1995 by ~25% from 12 to 9 (*42*). This decline was not included in our extrapolation of the C_2F_6 emissions from the aluminum industry and as a result our estimated emissions are biased to lower values. Taking this estimate of the C_2F_6 emissions and comparing it to the total estimated emissions, determined from the later trend in Figure 3, gives an estimate of the contribution of the semiconductor industry to global C_2F_6 emissions (Figure 4b). As a result of the bias in the estimated C_2F_6 emissions from the aluminum industry, these estimated emissions from the semiconductor industry should be interpreted as upper limits.

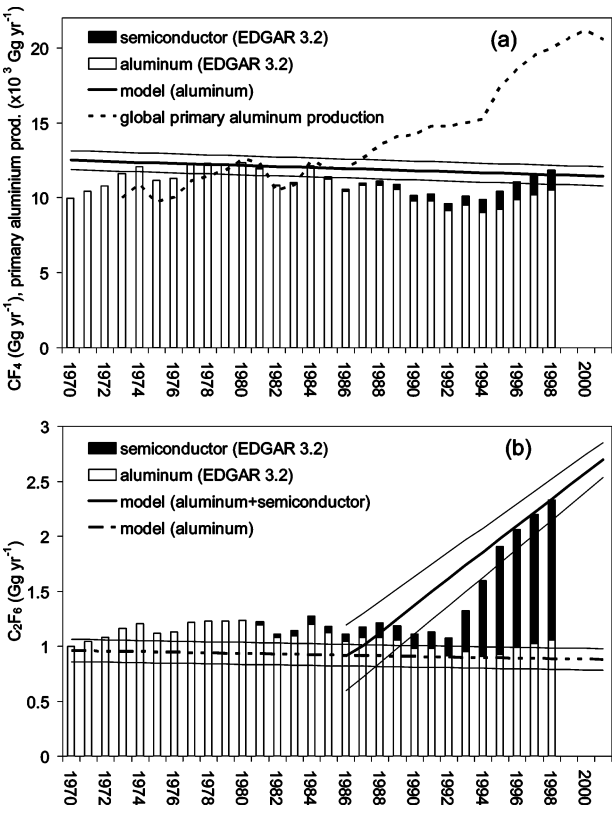

FIGURE 4. Combined emissions of (a) CF_4 and (b) C_2F_6 from the aluminum (empty bars) and semiconductor (solid bars) industries for the period 1970−1998 as estimated by EDGAR (*41*). The estimated CF_4 emissions as predicted from the firn air modeling for 1970−2001 (solid black line) and the trend in global primary aluminum production for the period 1970−2001 (*23*) (dashed black line) are shown in panel a. The estimated emissions of C_2F_6 from the aluminum and semiconductor industries (solid black line) and just the aluminum industry (dashed black line), as determined from the extrapolation of the early slope of CF_4:C_2F_6 (Figure 3), are shown as a dashed line in panel b. The solid gray lines show the estimated uncertainties in these emission estimates derived from the errors in (i) the reconstructed CF_4 trend and (ii) both CF_4:C_2F_6 ratios (Figure 3).

Our estimates differ from those of EDGAR although both show increasing trends between the late 1980s and 1998. Our results show a constant linear increase from ~1986, as a result of the nature of the employed methodology, as opposed to EDGAR which shows a more rapid increase after 1992. These estimates would suggest that emissions of CF_4 and C_2F_6 from the aluminum industry (assuming a negligible contribution of CF_4 from the semiconductor industry) for the period 1970−2001 were reasonably stable at 12 ± 0.5 and 0.92 ± 0.04 Gg yr^{-1}, respectively. Over the same time frame global primary aluminum production has continued to increase, most notably between 1994 and 1998 (~30%) (Figure 4a), implying that the CF_4 and C_2F_6 emission factors for the aluminum industry are declining, in agreement with industry reports (*15*, *16*, *40*).

These estimates also suggest that C_2F_6 emissions from the semiconductor industry have increased from 0.47 ± 0.21 to 1.8 ± 0.11 Gg yr^{-1} between 1990 and 2001. The agreement in the magnitude of the estimated emissions from EDGAR and this work is encouraging. The total C_2F_6 emissions of 2.7 ± 0.16 Gg in 2001 are considerably higher than the standard

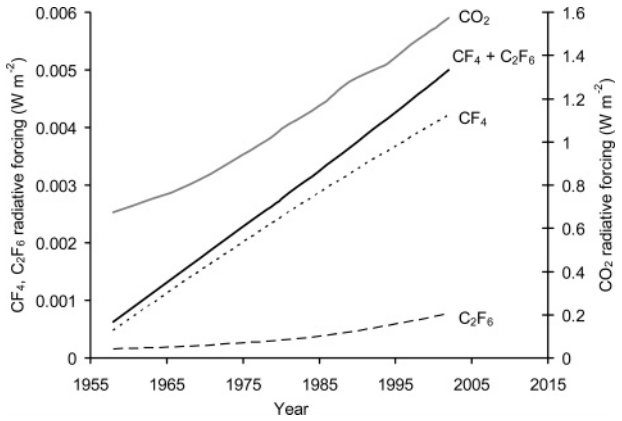

FIGURE 5. Time history of the global annual mean radiative forcings for CF_4 (dotted line), C_2F_6 (dashed line), and the sum of CF_4 and C_2F_6 (solid black line) relative to that of CO_2 (solid gray line).

IPCC Special Report on Emission Scenarios (SRES) (*43*) value of 1.3 Gg for 2000, and our data and the EDGAR data do not support the SRES assumption of a decrease from 1.6 Gg yr^{-1} to 1.3 Gg yr^{-1} between 1990 and 2000. Similarly, SRES projects a decrease in CF_4 emissions from 16 Gg yr^{-1} to 13 Gg yr^{-1} between 1990 and 2000, which is much greater than the decrease derived here (Figure 4a), although the SRES value in 2000 is similar to the EDGAR and our 2001 value.

The time history of the radiative forcings, i.e., the perturbation resulting from the concentration change between the preindustrial (taken as the year 1750) and a given year, of CF_4 and C_2F_6 are shown in Figure 5. The time history of atmospheric concentrations were provided on a global basis from a 2D chemistry transport model (*36*) using the firn air measurements of CF_4 and C_2F_6. In this method of estimating the radiative forcing, the radiative forcing varies linearly with the atmospheric concentration, and therefore, the trend in radiative forcing with time of the two gases was similar to that of the atmospheric concentration time trend. The radiative forcing for CF_4 increases steadily after 1960 with a slight decrease in trend after 1990. The radiative forcing of C_2F_6 shows a steady increase until the 1980s where it rapidly increases.

The radiative forcings of CF_4 and C_2F_6 are small in magnitude when compared to the major greenhouse gases: 0.3, 1, and 3% of carbon dioxide (CO_2) (Figure 5), methane (CH_4), and nitrous oxide (N_2O) (not shown), respectively. However, the CF_4 and C_2F_6 forcings are essentially irreversible as a result of their long atmospheric lifetimes (Table 1). The CO_2 (Figure 5), CH_4, and N_2O radiative forcings (not shown) were calculated using mixing ratios from the Goddard Institute for Space Science (GISS) (*44*) and the reported IPCC (*35*) formula for the gases.

The 1998 estimate for the radiative forcing of CF_4 is 3.9 $\times 10^{-3}$ Wm^{-2} and that of C_2F_6 is 6.7 $\times 10^{-4}$ Wm^{-2}. The IPCC estimates, for the same year, are 3.0 $\times 10^{-3}$ Wm^{-2} and 1.0 $\times 10^{-3}$ Wm^{-2} for CF_4 and C_2F_6, respectively (*35*). The differences are due to a combination of the discrepancies in the radiative efficiencies calculated here and those quoted in the IPCC 2001 report (*35*) and the differences in the atmospheric concentrations estimated for 1998 between this study and the IPCC 2001 report (*35*). Multiplying the year 2000 emissions (Figure 4) by the 100 year GWPs (Table 1) yields total CF_4 and C_2F_6 CO_2-equivalent emissions of about 110 Mt—or about 0.5% of the fossil-fuel CO_2 emissions in that year (*35*). Using the IPCC (*35*) values for both the year 2000 emissions and the GWPs would yield CO_2-equivalent emissions almost 25% smaller.

Acknowledgments

This work was funded by the CEC program (EUK2-CT2001-00116, CRYOSTAT). The North GRIP project is directed and organized by the Department of Geophysics at the Niels Bohr Institute for Astronomy, Physics and Geophysics, University of Copenhagen. It is supported by Funding Agencies in Denmark (SNF), Belgium (FNRS-CFB), France (IFRTP and INSU/CNRS), Germany (AWI), Iceland (RannIs), Japan (MEXT), Sweden (SPRS), Switzerland (SNF), and the United States of America (NSF). The Berkner Island drilling was organized and conducted by the British Antarctic Survey with funding from the Natural Environmental Research Council (NERC). D.R.W. acknowledges NERC for Ph.D. studentship funding.

Supporting Information Available

More detailed descriptions of the analytical methods, calibration procedure, and the iterative modeling methodology. This material is available free of charge via the Internet at http://pubs.acs.org.

Literature Cited

(1) Oram, D. E. Trends of long-lived anthropogenic halocarbons in the Southern Hemisphere and model calculations of global emissions. Ph.D. Thesis, School of Environmental Sciences, University of East Anglia, Norwich, U.K, 1999.

(2) Harnisch, J.; Borchers, R.; Fabian, P.; Maiss, M. CF_4 and the age of mesospheric and polar vortex air. *Geophys. Res. Lett.* **1999**, *26*, 295−298.

(3) Khalil, M. A. K.; Rasmussen, R. A.; Culbertson, J. A.; Prins, J. M.; Grimsrud, E. P.; Shearer, M. J. Atmospheric perfluorocarbons. *Environ. Sci. Technol.* **2003**, *37*, 4358−4361.

(4) Harnisch, J.; Borchers, R.; Fabian, P.; Maiss, M. Tropospheric trends for CF_4 and C_2F_6 since 1982 derived from SF_6 dated stratospheric air. *Geophys. Res. Lett.* **1996**, *23*, 1099−1102.

(5) Roehl, C. M.; Boglu, D.; Bruhl, C.; Moortgat, G. K. Infrared band intensities and global warming potentials of CF_4, C_2F_6, C_3F_8, C_4F_{10}, C_5F_{12}, and C_6F_{14}. *Geophys. Res. Lett.* **1995**, *22*, 815−818.

(6) Highwood, E. J.; Shine, K. P. Radiative forcing and global warming potentials of 11 halogenated compounds. *J. Quant. Spectrosc. Radiat. Transf.* **2000**, *66*, 169−183.

(7) Hurley, M. D.; Wallington, T. J.; Buchanan, G. A.; Gohar, L. K.; Marston, G.; Shine, K. P. IR spectrum and radiative forcing of CF_4 revisited. *J. Geophys. Res.* **2005**, *110*, 1−8.

(8) Montzka, S. A.; Fraser, P. J., (lead authors); Butler, J. H.; Connell, P. S.; Cunnold, D. M.; Daniel, J. S.; Derwent, R. G.; Lal, S.; McCulloch, A.; Oram, D. E.; Reeves, C. E.; Sanhueza, E.; Steele, L. P.; Velders, G. J. M.; Weiss, R. F.; Zander, R. J. Controlled substances and other source gases, Chapter 1. In *Scientific Assessment of Ozone Depletion 2002*; Global Ozone Research and Monitoring Project; World Meteorological Organization: Geneva, Switzerland, 2003.

(9) Ravishankara, A. R.; Solomon, S.; Turnipseed, A. A.; Warren, R. F. Atmospheric lifetimes of long-lived halogenated species. *Science* **1993**, *259*, 194−199.

(10) Morris, R. A.; Miller, T. M.; Viggiano, A. A.; Paulson, J. F.; Solomon, S.; Reid, G. Effects of electron and ion reactions on atmospheric lifetimes of fully fluorinated compounds. *J. Geophys. Res.* **1995**, *100*, 1287−1294.

(11) Cicerone, R. J. Atmospheric carbon tetrafluoride: a nearly inert gas. *Science* **1979**, *206*, 59−61.

(12) Penkett, S. A.; Prosser, N. J. D.; Rasmussen, R. A.; Khalil, M. A. K. J. Atmospheric measurements of CF_4 and other fluorocarbons containing the CF_3 grouping. *J. Geophys. Res.* **1981**, *86*, 5172−5178.

(13) United States Environmental Protection Agency: Inventory of U.S. greenhouse gas emissions and sinks 1990−2004. http://yosemite.epa.gov/oar/globalwarming.nsf/UniqueKeyLookup/RAMR6MBLPN/$File/06Industrial.pdf, 2006.

(14) Gibbs, M. J.; Bakshi, V.; Lawson, K.; Pape, D. *Good practice guidance and uncertainty management in national greenhouse gases: Chapter 3.3 - PFC emissions from primary aluminium production*; www.ipcc-nggip.iges.or.jp/public/gp/english; IPCC, 2000.

(15) IAI. *Perfluorocarbon emissions reduction programme 1990−2000*; International Aluminium Institute: London, 2001.

(16) IAI. *Anode effect survey 1994−1997 and perfluorocarbon compounds emission survey 1990−1997*; International Aluminium Institute: London, 2000.
(17) Bartos, S. C.; Burton, C. S. *Good practice guidance and uncertainty management in national greenhouse gases: Chapter 3.8 - PFC. HFC, NF_3 and SF_6 emissions from semiconductor manufacturing*; www.ipcc-nggip.iges.or.jp/public/gp/english; IPCC, 2000.
(18) Harnisch, J.; Borchers, R.; Fabian, P.; Gaggeler, H. W.; Schotterer, U. Effect of natural tetrafluoromethane. *Nature* **1996**, *384*, 32.
(19) Harnisch, J.; Eisenhauer, A. Natural CF_4 and SF_6 on Earth. *Geophys. Res. Lett.* **1998**, *25*, 2401−2404.
(20) Harnisch, J.; Frische, M.; Borchers, R.; Eisenhauer, A.; Jordan, A. Natural fluorinated organics in fluorite and rocks. *Geophys. Res. Lett.* **2000**, *27*, 1883−1886.
(21) Fabian, P.; Borchers, R.; Kruger, B. C.; Lal, S. CF_4 and C_2F_6 in the atmosphere. *J. Geophys. Res.* **1987**, *92*, 9831−9835.
(22) Jordan, A.; Harnisch, J.; Borchers, R.; Le, Guern, F. N.; Shinohara, H. Volcanogenic halocarbons. *Environ. Sci. Technol.* **2000**, *34*, 1122−1124.
(23) IAI. *Primary Aluminium Production, Current IAI statistics*; International Aluminium Institute: London, 2006; www.world-aluminium.org.
(24) Worton, D. R.; Sturges, W. T.; Schwander, J.; Mulvaney, R.; Barnola, J.-M.; Chappellaz, J. 20th century trends and budget implications of chloroform and other related tri- and dihalomethanes inferred from firn air. *Atmos. Chem. Phys.* **2006**, *6*, 1−17.
(25) Mulvaney, R.; Oerter, H.; Peel, D. A.; Graf, W.; Arrowsmith, C.; Pasteur, E. C.; Knight, B.; Littot, G. C.; Miners, W. D. 1000 year ice-core records from Berkner Island, Antarctica. *Ann. Glaciol.* **2002**, *35*, 45−51.
(26) Sturges, W. T.; McIntyre, H. P.; Penkett, S. A.; Chappellaz, J.; Barnola, J. M.; Mulvaney, R.; Atlas, E.; Stroud, V. Methyl bromide, other brominated methanes, and methyl iodide in polar firn air. *J. Geophys. Res.* **2001**, *106*, 1595−1606.
(27) Schwander, J.; Barnola, J. M.; Andrie, C.; Leuenberger, M.; Ludin, A.; Raynaud, D.; Stauffer, B. The Age of the Air in the Firn and the Ice at Summit, Greenland. *J. Geophys. Res.* **1993**, *98*, 2831−2838.
(28) Oram, D. E.; Reeves, C. E.; Penkett, S. A.; Fraser, P. J. Measurements of HCFC-142b and HCFC-141b in the Cape-Grim Air Archive 1978−1993. *Geophys. Res. Lett.* **1995**, *22*, 2741−2744.
(29) Fraser, P. J.; Oram, D. E.; Reeves, C. E.; Penkett, S. A.; McCulloch, A. Southern Hemispheric halon trends (1978−1998) and global halon emissions. *J. Geophys. Res.* **1999**, *104*, 15985−15999.
(30) Lee, J. Determination of stratospheric lifetimes of HCFC's and other halogenated hydrocarbons from balloon-bourne profile measurements. Ph.D. thesis, University of East Anglia, Norwich, U.K., 1994.
(31) Trudinger, C. M.; Etheridge, D. M.; Rayner, P. J.; Enting, I. G.; Sturrock, G. A.; Langenfelds, R. L. Reconstructing atmospheric histories from measurements of air composition in firn. *J. Geophys. Res.* **2002**, *107*, art. no.-4780.
(32) Rommelaere, V.; Arnaud, L.; Barnola, J. M. Reconstructing recent atmospheric trace gas concentrations from polar firn and bubbly ice data by inverse methods. *J. Geophys. Res.* **1997**, *102*, 30069−30083.
(33) Fabre, A.; Barnola, J. M.; Arnaud, L.; Chappellaz, J. Determination of gas diffusivity in polar firn: comparison between experimental measurements and inverse modeling. *Geophys. Res. Lett.* **2000**, *27*, 557−560.
(34) Fuller, E. N.; Schettle, P. D.; Giddings, J. C. A new method for prediction of binary gas phase diffusion coeffecients. *Ind. Eng. Chem.* **1966**, *58*, 19−27.
(35) Houghton, J. T.; Ding, Y.; Griggs, D. J.; Noguer, M.; van der Linden, P. J.; Xiaosu, D. *Climate change 2001: The scientific basis. Contribution of working group I to the third assessment of the intergovernmental panel on climate change (IPCC)*; Cambridge University Press: New York, 2001.
(36) Martinerie, P.; Brasseur, G. P.; Granier, C. The chemical composition of ancient atmospheres: a model study constrained by ice core data. *J. Geophys. Res.* **1995**, *100*, 14291−14304.
(37) Sihra, K.; Hurley, M. D.; Shine, K. P.; Wallington, T. J. Updated radiative forcing estimates of sixty-five halocarbons and non-methane hydrocarbons, *J. Geophys. Res.* **2001**, *106*, 20493−20506.
(38) Geller, L. S.; Elkins, J. W.; Lobert, J. M.; Clarke, A. D.; Hurst, D. F.; Butler, J. H.; Myers, R. C. Tropospheric SF_6: observed latitudinal distribution and trends, derived emissions and interhemispheric exchange time. *Geophys. Res. Lett.* **1997**, *24*, 675−678.
(39) Maiss, M.; Brenninkmeijer, C. A. M. Atmospheric SF_6: trends, sources, and prospects. *Environ. Sci. Technol.* **1998**, *32*, 3077−3086.
(40) IAI. *The international aluminium institute's report on the aluminium industry's global perfluorocarbon gas emissions reduction programme - results of the 2003 anode effect survey*; International Aluminium Institute: London, 2005.
(41) Olivier, J. G. J.; Berdowski, J. J. M.; Peters, J. A. H. W.; Bakker, J.; Visschedijk en, A. J. H.; Blos, J.-P. J. Applications of EDGAR. Including a description of EDGAR 3.0: reference database with trend data for 1970−1995. RIVM report no. 773301001/NOP report no. 410200 051; RIVM: Bilthoven, The Netherlands, 2001.
(42) Harnisch, J. *Emission Scenarios for CF_4 and C_2F_6 derived from reconstructed atmospheric concentrations: Proceedings of EPA workshop on a successful partnership to reduce PFC emissions from primary aluminium production*; United States Environmental Protection Agency: Washington, D.C.,1996.
(43) Nakicenovic, N.; Alcamo, J.; Davis, G.; de Vries, B.; Fenhann, J.; Gaffin, S.; Gregory, K.; Grübler, A.; Yong Jung, T.; Kram, T.; Lebre La Rovere, E.; Michaelis, L.; Mori, S.; Morita, T.; Pepper, W.; Pitcher, H.; Price, L.; Riahi, K.; Roehrl, A.; Rogner, H-H.; Sankovski, A.; Schlesinger, M.; Shukla, P.; Smith, S.; Swart, R.; van Rooijen, S.; Victor, N.; Dadi, Z. *Emission Scenarios 2000. Special report of the intergovernmental panel on climate change (IPCC)*; Cambridge University Press: New York, 2001.
(44) Goddard Institute for Space Science (GISS). *Well mixed anthropogenic greenhouse gases*; http://www.giss.nasa.gov/data/simodel/ghgases/, 2006.

Received for review July 18, 2006. Revised manuscript received January 16, 2007. Accepted January 22, 2007.

ES061710T